Ionospheric Research

NASA Grant NGR 39-009-032

Scientific Report

on

"A Time-of-Flight Mass Spectrometer Suitable for Ionospheric Composition Investigations"

by

H. T. Diem

September 25, 1967

Scientific Report No. 309

Ionosphere Research Laboratory

Submitted by: B. R. F. Kendall
B. R. F. Kendall, Associate Professor of Physics

Approved by: A. H. Waynick
A. H. Waynick, Professor of Electrical Engineering,
Director, Ionosphere Research Laboratory

The Pennsylvania State University

College of Engineering

Department of Electrical Engineering

TABLE OF CONTENTS

ABSTRACT

A small sensitive time-of-flight mass spectrometer is being developed which appears to fulfill the necessary requirements for an ionospheric probe. The instrument's small size and light weight along with its high sensitivity and ability to operate at relatively high pressures make it a desirable tool for investigating the ion composition of the D and E regions of the ionosphere. Preliminary results are discussed.

CHAPTER I

INTRODUCTION

1.1 Application of Mass Spectrometers to Ionospheric Composition Investigations

During the past fifteen years much work has been done utilizing mass spectrometers to investigate ionospheric particle composition. The basic type of instruments used in ionospheric rocket probes to date have been the Bennett rf mass spectrometer, the quadrupole mass filter, pulsed-beam time-of-flight spectrometers, and small magnetic sector spectrometers.

Early experiments of Johnson and coworkers (1955-1958) used Bennett-type rf spectrometers which sampled the mass spectrum between 5 amu and 48 amu once per second with a resolving power of 25. Data was obtained at altitudes ranging from 100 km to 160 km.

Sayers (1959) has described a large-aperture time-of-flight mass spectrometer of cylindrical geometry which was subsequently flown by MacKenzie (1964). This instrument operated at altitudes ranging from 90 km to 160 km. The dimensions of this instrument were rather large for a flyable mass spectrometer and a fairly large rocket was required to fly it.

Narcisi and coworkers (1965) have successfully flown a quadrupole mass filter capable of determining the ion composition of the D region of the ionosphere, i.e. altitudes from 60 km to 100 km. The use of

quadrupole spectrometers for low altitude rocket probes requires the employment of liquid-nitrogen-chilled zeolite pumps to reduce the instrument pressure to its operating range. Narcisi was able to make measurements starting at 60 km and in the early work a resolving power of 16 was obtained.

Hoffman (1965) has developed a 1.5 inch 60 degree sector-field mass spectrometer suitable for ion composition investigations utilizing high altitude rockets and satellites. This instrument has been designed primarily for the investigation of the F_1 and F_2 regions encompassing altitudes from 200 km up.

In addition to the ion composition investigations mentioned above, Schaeffer (1963) has flown a quadrupole mass filter with an ionization source in order to investigate neutral particle composition between 95 km and 135 km. Nier and coworkers (1965) have used a 90 degree magnetic sector spectrometer to study neutral composition between 100 km and 200 km. This instrument is capable of detecting masses in the range 2 amu to 50 amu. Sputter pumps are used to reduce the instrument pressure to operable levels.

1.2 Advantages of Using a Pulsed-Beam Time-of-Flight Mass Spectrometer for Ionospheric Investigation

The basic requirements of any mass spectrometer intended for airborne ion composition investigations are as follows: The spectrometer should exhibit simplicity of design and construction in order to insure reliability. The associate electronic circuitry should also be simple and reliable. Due to the size and weight limitations inherent in an airborne probe, the spectrometer must be small in physical size. A time-of-flight mass spectrometer can be constructed which fulfills all of the above requirements.

The more fundamental problems involved in designing a pulsed beam mass spectrometer capable of yielding useful information about the D region of the ionosphere can also be resolved. During the daytime the negative ion concentrations in the D region are expected to be much smaller than the positive ion concentrations. The pulsing region of a time-of-flight mass spectrometer may be made large enough that its ion gathering capacity will be sufficient for both positive and negative ion composition investigations. It always is possible to fly an electron bombardment ion source in conjunction with a spectrometer of this nature and hence neutral particle investigations are possible. A time-of-flight mass spectrometer may be constructed which will operate at the high pressures

involved in D region experiments. The ion flight path of the spectrometer may be made sufficiently short to reduce particle collisions at these high pressures.

The small size of an instrument of this nature yields even further advantages. It will be possible to use two or more of these spectrometers in one rocket probe utilizing the same electronic systems. This would increase the reliability of a given experiment and provide cross checks of the performance of each instrument. In addition, it will be possible to utilize small inexpensive rockets for individual probes.

It is necessary to point out that the major disadvantage of time-of-flight spectrometers used in atmospheric investigation is the limited resolving power of the instrument. The size requirements of an airborne instrument preclude the possibility of incorporating a long ion flight path in the spectrometer. This limits the maximum attainable resolving power. Kendall (1961, 1962, and 1966) and Zabielski (1966), have shown that it is possible to increase the effective instrument resolving power by a factor of six or more utilizing analog data processing methods. Hence devices of low resolution but high sensitivity can be quite useful in determining ionospheric constituents.

1.3 Survey of Major Work on Time-of-Flight Mass Spectrometers

As a consequence of the major electronic advances brought about by World War II, the pulsed beam time-of-flight mass spectrometer became feasible. The instrument was first proposed by Stephens (1944) and models were constructed by Cameron and Eggers (1945), by Keller (1949), by Takekoshi (1951), and by Wolff and Stephens (1953). These instruments all operated on the principle that ions of given energy and different mass to charge ratios require different times to traverse a given distance. The instruments mentioned above were severely limited in resolving power[1] because of poor space focusing properties and relatively poor frequency response of the amplifiers used in the detecting circuits. There have been several major improvements to time-of-flight mass spectrometers and some of these will be discussed below.

Glenn (1951 and 1952) constructed an instrument in which the ions are subjected to an rf sawtooth voltage and a dc accelerating potential. This spectrometer consists basically of an ion source, bunching grids, gating grids, and detection apparatus. The ions are accelerated to the bunching grids by a dc potential. This accelerating field is of such a nature that the time the ions spend between the bunching grids is short in comparison to the

[1]See Section 5.30.

period of voltage change on the bunching grids. It may be shown that those ions homogeneous in mass to charge ratio will arrive at the gating grids at a precise instant in time independent of the time they leave the bunching grids if the voltage on the buncher grid increases linearly with time. Ions which travel through the buncher grid first receive less energy than those moving through the buncher grid at some later instant in time. The appropriate waveform for the buncher grid is thus an rf sawtooth voltage. The bunched ions arrive at a gate grid and at the appropriate time a pulse is applied which accelerates the ion bunch toward the collector. This gate pulse insures that all ions which do not have the appropriate flight time do not reach the collector.

Katzenstein and Friedland (1955) also showed that improved signal to noise ratio was possible if one used a gated collector system. The gate permits observation of only one mass at a time and it is possible to integrate the ion current corresponding to any mass over a large number of pulses. Since the signal adds arithmetically and the noise adds randomly, the signal to noise ratio is much improved. It was possible to scan the mass spectrum comparatively slowly, resulting in good resolution between adjacent mass peaks in spite of the then existing low bandpass amplifiers.

Wiley and McLaren (1955) obtained improved resolving power by redesigning the ion gun or source region. The ion gun contains two distinct accelerating regions which makes possible the focusing of the initial space distribution of the ions under investigation. The resolving power of a time-of-flight mass spectrometer depends on its ability to reduce the time spread caused by the initial space and energy distributions of ions under formation. The space focusing of this instrument depends upon the fact that an ion formed initially closer to the detector acquires less energy than an ion formed close to the pulsed grid. Hence the ion formed close to the pulsed grid will eventually overtake an ion formed closer to the detector. It is possible to obtain an expression for the point where two ions of given charge to mass ratio will overtake each other. The collector is then located at this point and space focusing is achieved. It is also possible to minimize the effects of the initial velocity spread of ions undergoing formation. This is accomplished by adjusting the grid spacings in the source.

At about the same time Agishev and Ionov (1956) described an instrument almost identical in principle to that of Wiley and McLaren. They improved a gated mass spectrometer described earlier by Ionov and Mamyrin (1953) which incorporated what was essentially a double field source. The spectrometer of Ionov and Mamyrin

developed a resolving power of about 55, whereas the spectrometer of Agishev and Ionov developed a resolving power comparable to that of Wiley and McLaren, about 200. These instruments have the advantage that the mass spectrum may be scanned very rapidly and a visual record is available in the form of a trace on an oscilloscope. The resolution is limited mainly by the electronics of the collector system.

Borovik and Grishin (1959) have shown that it is possible to increase the sensitivity of the double field time-of-flight mass spectrometer by increasing the cross sectional area of the ion beam. In order to increase the ionic current, the dimensions of the grids were made sufficiently large so that the cross section of the ionic beam was 36 cm^2. The resolving power of this instrument was not greater than 10.

Sakseev (1965) has shown that it is possible to construct a small time-of-flight mass spectrometer utilizing the double field ion source which will operate at relatively high pressures, i.e. up to 1×10^{-3} torr. The resolving power of this device was about 25.

CHAPTER II

STATEMENT OF PROBLEM

The specific problem is the development of a small, sensitive time-of-flight mass spectrometer capable of yielding information concerning positive and negative ion concentrations in the D and E regions of the ionosphere. This thesis describes a mass spectrometer of wedge-shaped geometry which fulfills the above requirements. It is also shown that this spectrometer has advantages over previous spectrometers which have been used in similar investigations.

CHAPTER III

THEORY OF OPERATION

3.1 The Linear Pulsed-Beam Mass Spectrometer

The convention which will be followed in labeling the grids of any mass spectrometer described in this thesis is as follows. All grids will be numbered from source to collector with successive grids labeled with increasing numbers.

The linear pulsed-beam time-of-flight mass spectrometer as developed by Wiley and McLaren is illustrated in Figure 1. While the ions are being formed by electron bombardment between grids 1 and 2 the potentials on the two grids are approximately equal. The second region, between grids 2 and 3, has a constant electric field E_d and the region D is field free. Ions are accelerated out of the region between 1 and 2 by a pulse applied to 1. The total time taken for an ion formed at the point s having charge q and mass m to traverse the length of the spectrometer will be

$$T = T_s + T_d + T_D \qquad (1)$$

where T_s is the time taken for the ion to travel from point s to the grid 2, and T_d and T_D are the times the ion spends in the regions d and D respectively. Suppose V_s is the electric potential at the point s, relative to the

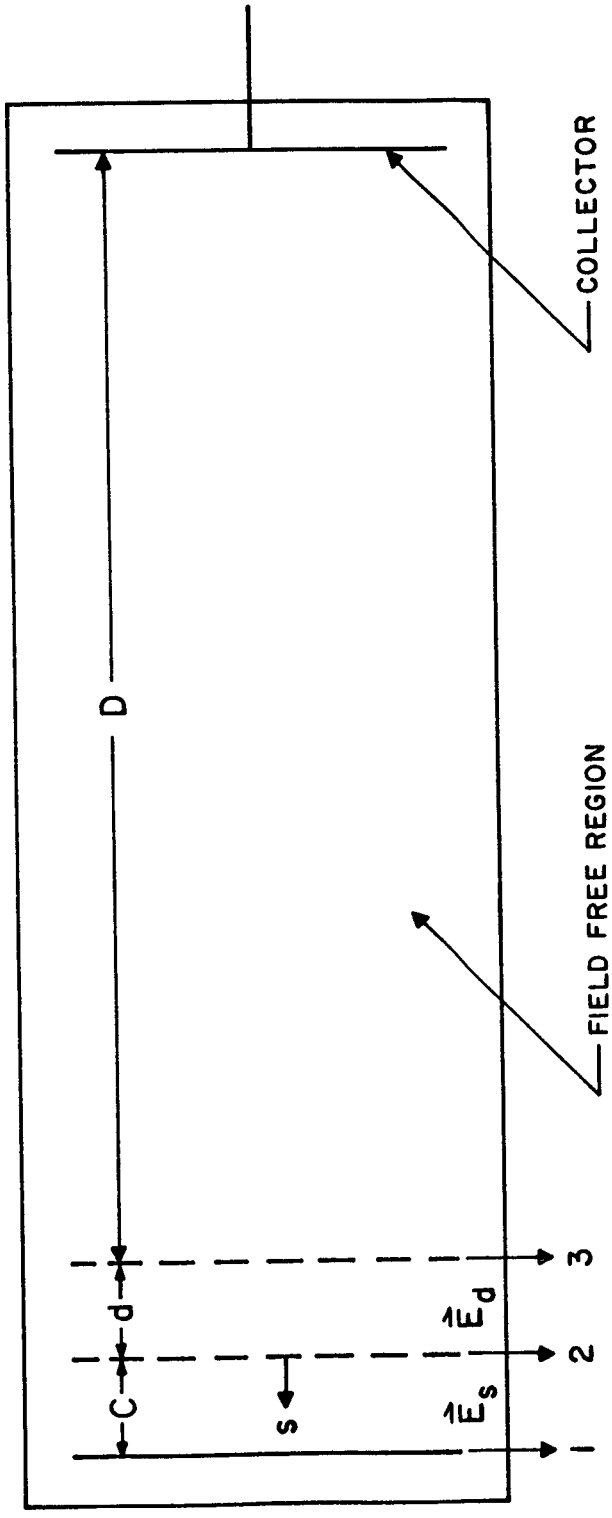

LINEAR PULSED-BEAM MASS SPECTROMETER AFTER WILEY AND McLAREN (1955)

FIGURE 1

potential of grid 2, when the pulse is applied. Then an ion formed at s will experience a force

$$m \frac{d^2x}{dt^2} = \frac{qV_s}{s} = \frac{U_s}{s} \tag{2}$$

where U_s is the energy gained by the ion in moving through the distance s. Hence

$$\frac{d^2x}{dt^2} = \frac{1}{ms} U_s \tag{3}$$

and

$$\frac{dv}{dt} = \frac{1}{ms} U_s \tag{4}$$

Equation 4 may be integrated from v_0 to v_s where v_0 is the velocity of the ion. We then have

$$\int_{v_o}^{v_s} dv = \frac{U_s}{ms} \int_{o}^{T_s} dt. \tag{5}$$

Equation 5 yields

$$v_s \pm v_o = \frac{1}{ms} U_s T_s \tag{6}$$

The $\pm$ sign indicates that the ion may have a component of velocity in either the positive or negative direction.

From Equation 6 we have

$$v_s = \frac{1}{ms} U_s T_s \pm \left(\frac{2U_o}{m}\right)^{1/2} \tag{7}$$

where U_o is the initial energy of formation of the ion, or the energy due to the relative motion of the spectrometer and ion. Performing another integration of Equation 7,

$$\int_o^s dx = \frac{1}{ms} U_s \int_o^{T_s} T dt \pm \left(\frac{2U_o}{m}\right)^{1/2} \int_o^{T_s} dt \tag{8}$$

we get

$$s = \frac{U_s}{2ms} T_s^2 \pm \left(\frac{2U_o}{m}\right)^{1/2} T_s, \tag{9}$$

Solving the quadratic equation for T_s we obtain

$$T_s = \frac{ms}{U_s} \left[\pm \left(\frac{2U_o}{m}\right)^{1/2} + \left(\frac{2U_o}{m} + \frac{2U_s}{m}\right)^{1/2} \right] \tag{10}$$

or

$$T_s = \frac{(2m)^{1/2}}{qE_s} \left[(U_o + U_s)^{1/2} \pm (U_o)^{1/2} \right] \tag{11}$$

where E_s is the electric field between grids 1 and 2. In an analogous manner one may show that for the region between grids 2 and 3,

$$T_d = \frac{(2m)^{1/2}}{qE_d} \left[(U)^{1/2} - (U_o + U_s)^{1/2} \right] \tag{12}$$

where U is the total energy, i.e.

$$U = U_o + qsE_s + gdE_d. \tag{13}$$

Since the electric field is zero in the region D we have

$$T_D = \frac{D}{v_d} \tag{14}$$

and

$$v_d = \left(\frac{2U}{m}\right)^{1/2} \tag{15}$$

hence

$$T_d = D\left(\frac{m}{2U}\right)^{1/2}. \tag{16}$$

Space focusing is independent upon the fact that an ion formed initially closer to 2 acquires less energy than an ion formed close to 1. Hence the ion formed close to 1 will eventually overtake an ion formed close to 2. In order to investigate the space focusing for fixed grid spacings, perhaps those suitable for a flyable mass spectrometer, we assume that there is no initial energy spread. In this case Equation 1 becomes

$$T = \left(\frac{2m}{q}\right)^{1/2}\left\{\frac{s}{\sqrt{V_s}} + \frac{d}{V_d}\left[(V_s+V_d)^{1/2} - (V_s)^{1/2}\right] + \frac{D}{2(V_s+V_d)^{1/2}}\right\} \tag{17}$$

where V_s+V_d and V_d are the potentials at point s and grid 2 respectively. Let the distance between grids 1

and 2 of Figure 1 be .48 cm, the distance between grids 2 and 3 be .48 cm, and the distance between grid 3 and the collector be 4.12 cm. We now locate three ions of the same mass to charge ratio in the pulsing region at the points $s_0-\Delta s$, s_0, and $s_0 + \Delta s$ where s_0 is .24 cm and Δs is .16 cm. We wish to investigate the difference in flight times of these ions as a function of the ratio of voltages on grids 1 and 2 when the pulse is applied. Three time differences are defined as follows,

$$\Delta T_1 = T_1 - T_2 \tag{18}$$

$$\Delta T_2 = T_2 - T_3 \tag{19}$$

and

$$\Delta T_3 = T_1 - T_3 \tag{20}$$

T_1 is the time of flight of the ion located at $s_0-\Delta s$, T_2 is the time of flight of the ion located at s_0, and T_3 is the time of flight of the ion located at $s_0+\Delta s$. Figure 2 is a plot of these time differences as a function of the ratio of voltages on grids 1 and 2, V_1/V_2. The space focusing is clearly demonstrated and is best for a voltage ratio of 2.15/1.

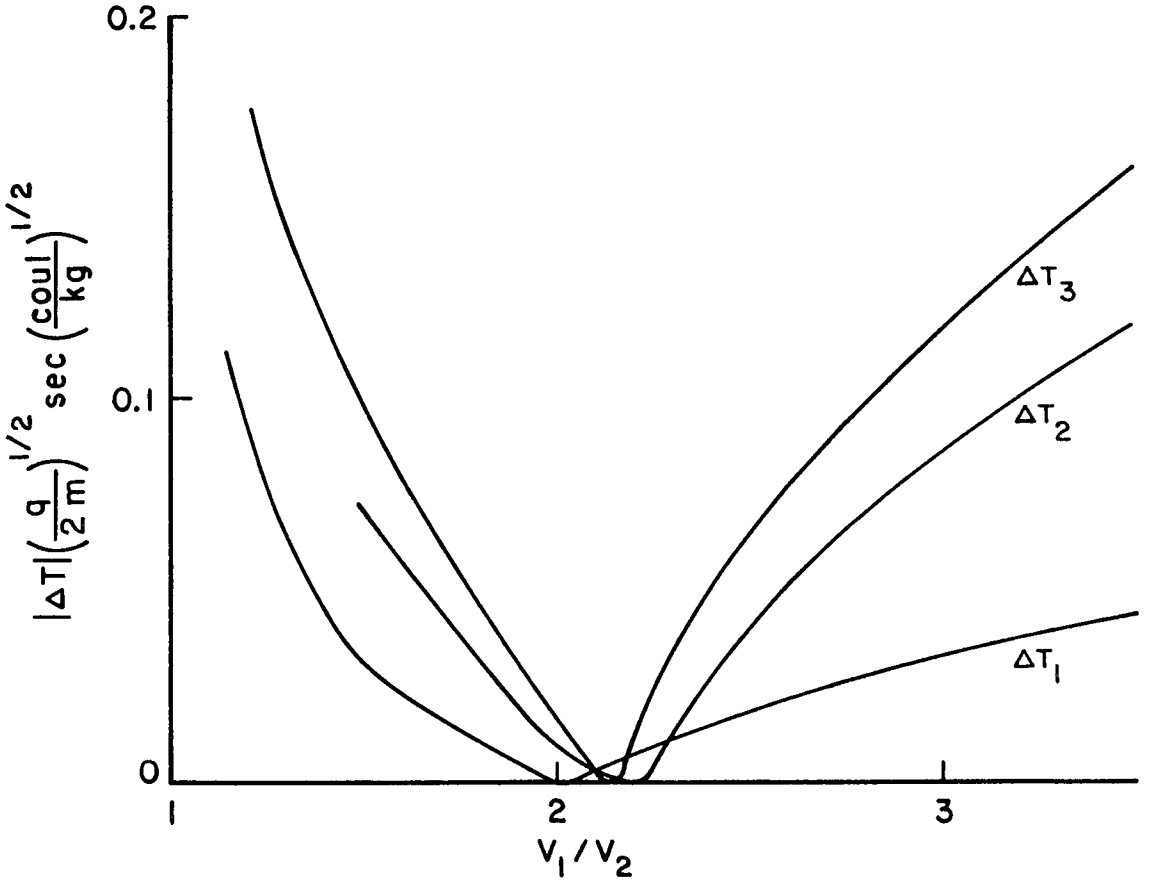

SPACE FOCUSING OF THE LINEAR PULSED-BEAM MASS SPECTROMETER

FIGURE 2

3.2 A Proposed Cylindrical Pulsed-Beam Mass Spectrometer

Figure 3 illustrates a top view of a proposed large-aperture cylindrical time of flight mass spectrometer. The device consists of three cylindrical grids and a fine wire collector. The problem of finding the time of flight of an ion introduced into the pulsing region directly through the first grid reduces to finding the solution to Laplace's equation

$$\vec{\nabla}^2 V = 0 \tag{21}$$

in cylindrical coordinates. The solution to Equation 21 for a cylindrical symmetric system is

$$\frac{dV}{dr} = \frac{A}{r} \tag{22}$$

where V is the electric potential at r and A is a constant. Integrating Equation 22 one obtains

$$V(r) = A\ln r + B \tag{23}$$

where B is a constant of integration. Applying the boundary conditions at r_a and r_b yields

$$V_a = A\ln r_a + B \tag{24}$$

and

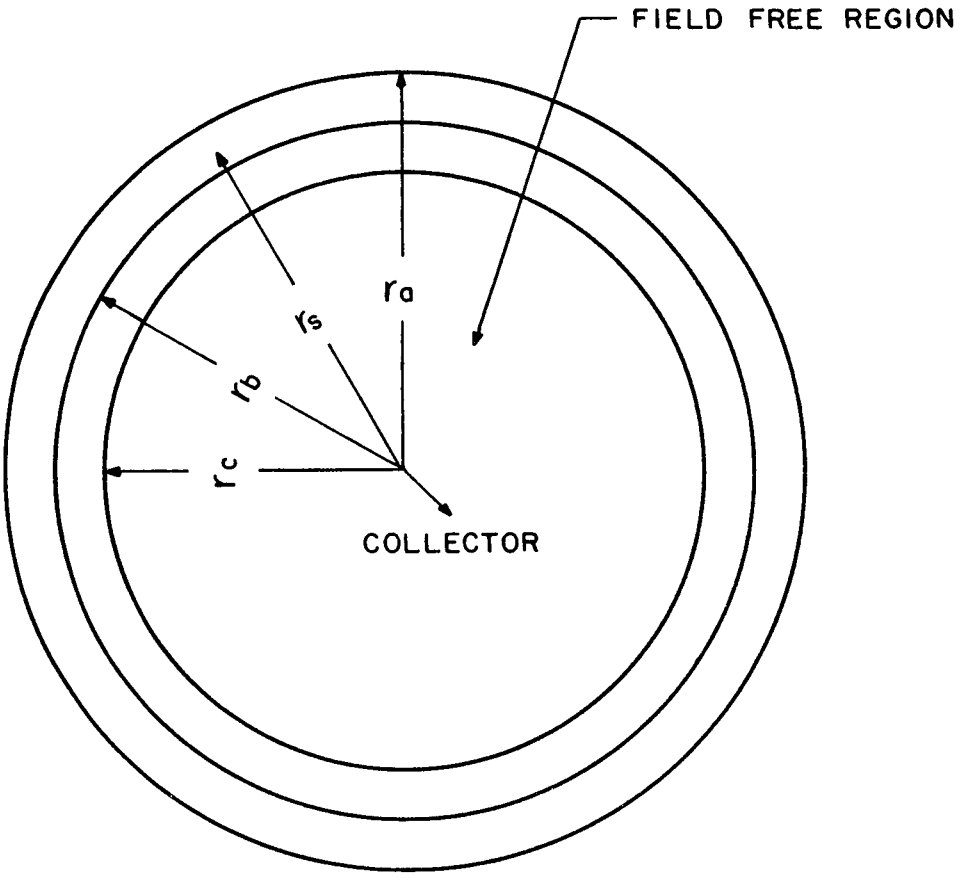

PROPOSED CYLINDRICAL PULSED-BEAM MASS SPECTROMETER

FIGURE 3

$$V_b = A\ln r_b + B \tag{25}$$

Solving these equations for the constants A and B yields

$$A = \frac{V_a - V_b}{\ln r_a/r_b} \tag{26}$$

and

$$B = V_a - \frac{(V_a - V_b)}{\ln r_a/r_b}\ln r_a \tag{27}$$

hence

$$V(r) = \frac{(V_a - V_b)}{\ln r_a/r_b} \ln \frac{r}{r_a} + V_a. \tag{28}$$

In the second region between r_b and r_c the potential is, analogously,

$$V(r) = \frac{(V_b - V_c)}{\ln r_b/r_c} \ln \frac{r}{r_b} + V_b. \tag{29}$$

If we assume that the grid located at r_c has a potential of zero volts then Equation 29 becomes

$$V(r) = \frac{V_b}{\ln r_b/r_c} \ln \frac{r}{r_b} + V_b. \tag{30}$$

Since the grid at r_c is at ground potential we have for the region between the third grid and the collector,

$$V(r) = 0. \tag{31}$$

In order to obtain the electric fields in each region, the gradients of Equations 28, 29, and 31, must be taken. For cylindrical symmetry it is only necessary to take the r component,

$$\vec{E} = -\vec{\nabla}_r V = -\frac{d}{dr} V. \tag{32}$$

Hence the field between r_a and r_b is found by using Equations 32 and 28 and is

$$E_1 = -\frac{(V_a - V_b)}{r \ln r_a/r_b} \tag{33}$$

Similarly for the second region

$$E_2 = -\frac{-V_b}{r \ln r_b/r_c} \tag{34}$$

and the third region

$$E_3 = 0 \tag{35}$$

It remains to find the total transit time of an ion of charge q and mass m subjected to the fields of Equations 33, 34, and 35. This time will be

$$T = T_1 + T_2 + T_3 \tag{36}$$

where T_1, T_2, and T_3 are the times the ion spends in each respective region. The equation of motion of an ion located at r_s, where $r_a > r_s > r_b$, is

$$m \frac{d^2r}{dt^2} = - \frac{q\ (V_s - V_b)}{r \ln r_s/r_b} \quad . \tag{37}$$

We now define a constant K by

$$K \equiv - \frac{q}{m} \frac{(V_s - V_b)}{\ln r_s/r_b} \tag{38}$$

and 37 becomes

$$\frac{d^2r}{dt^2} = K/r \quad . \tag{39}$$

We define P to be the radial velocity

$$P = \frac{dr}{dt} \quad . \tag{40}$$

Hence

$$\frac{d^2r}{dt^2} = \frac{dP}{dt} \tag{41}$$

and

$$\frac{dP}{dt} = \frac{dP}{dr} \frac{dr}{dt} \quad . \tag{42}$$

From Equations 41 and 42 we have

$$\frac{d^2r}{dt^2} = P \frac{dP}{dr} \tag{43}$$

and from Equations 39 and 43 we obtain

$$P \frac{dP}{dr} = K/r \tag{44}$$

Integrating Equation 44 we get

$$\frac{P^2}{2} = K\ln r + C \tag{45}$$

where C is the integration constant. If the ion is introduced into the spectrometer through the first grid and has an initial velocity component $|v_0|$ at the time the accelerating field E_1 is applied, then at time $t = 0$, $P = v_0$ at $r = r_s$. Applying these boundary conditions to Equation 45 we obtain

$$\frac{v_0^2}{2} = K\ln r_s + C \tag{46}$$

and

$$C = -K\ln r_s + \frac{v_0^2}{2} \tag{47}$$

hence

$$\frac{P^2}{2} = K\ln r/r_s + \frac{v_0^2}{2} \tag{48}$$

Using the definition of P and rearranging terms in Equation 48 yields

$$dt = \frac{dr}{(2K\ln r/r_s + v_0^2)^{1/2}} \tag{49}$$

and the integral is

$$T_1 = \frac{1}{\sqrt{2K}} \int_{r_s}^{r_b} \frac{dr}{(\ln r/r_s + \frac{v_0}{2K})^{1/2}} \qquad (50)$$

In order to evaluate this integral one makes the following substitutions:

$$x = \ln r/r_s$$

$$dr = r_s e^x dx$$

The integral becomes

$$T_1 = \frac{r_s}{\sqrt{2K}} \int_0^{\ln r_b/r_s} \frac{e^x dx}{(x + v_0^2/2K)^{1/2}} \qquad (51)$$

Equation 51 is evaluated by the further substitutions,

$$y = x + v_0^2/2K$$

$$dy = dx.$$

Hence we have

$$T_1 = \frac{r_s}{\sqrt{2K}} \int_{v_0^2/2K}^{\ln r_b/r_s + v_0^2/2K} \frac{\exp(y - \frac{v_0^2}{2K})}{y^{1/2}} dy \qquad (52)$$

and

$$T_1 = \frac{r_s \exp(-\frac{v_0^2}{2K})}{\sqrt{2K}} \int_{v_0^2/2K}^{\ln r_b/r_s + v_0^2/2} \frac{e^y}{y^{1/2}} dy. \qquad (53)$$

If the argument of 53 is expanded in a power series it

becomes

$$T_1 = \frac{r_s \exp\left(-\frac{v_0^2}{K}\right)}{\sqrt{2K}} \int_{v_0^2/2K}^{\ln r_b/r_s + v_0^2/2K} \sum_{n=0}^{\infty} \frac{y^{(n-1/2)}}{n!}\, dy. \tag{54}$$

The integration of 54 leads to

$$T_1 = \frac{r_s \exp\left(-\frac{v_0^2}{2K}\right)}{\sqrt{2K}} \sum_{n=0}^{\infty} \frac{1}{n!\,(n+1/2)} \left\{ \left(\ln r_b/r_s + \frac{v_0^2}{2}\right)^{n+1/2} - \left(\frac{v_0}{2K}\right)^{n+1/2} \right\} \tag{55}$$

which can be further simplified into

$$T_1 = \frac{r_s\, e^{\frac{v_0^2}{|2K|}}}{\sqrt{|2K|}} \sum_{n=0}^{\infty} \frac{(-1)^n}{n!\,(n+1/2)} \left\{ \left(\ln r_s/r_b + \frac{v_0^2}{|2K|}\right)^{n+1/2} - \left(\frac{v_0^2}{|2K|}\right)^{n+1/2} \right\} \tag{56}$$

by using the region $K = -|K|$ and factoring.

In the second region between r_b and r_c the equation of motion is

$$m\frac{d^2r}{dt^2} = -\frac{qV_b}{r \ln r_b/r_c}\,. \tag{57}$$

One defines the constant

$$L = -\frac{q}{m}\frac{V_b}{\ln r_b/r_c} \tag{58}$$

and the following equation becomes identical to equation 39,

$$\frac{d^2r}{dt^2} = L/r. \tag{59}$$

Using the same substitution as that used in 39, equation 39 becomes

$$\frac{P^2}{2} = L\ln r + D \tag{60}$$

The total energy the particle has gained at r_b is

$$\frac{1}{2}mv_b^2 = U_o + q(V_s - V_b) \tag{61}$$

hence

$$\frac{v_b^2}{2} = \frac{P_b^2}{2} = \frac{U_o}{m} + \frac{q(V_s - V_b)}{m} \tag{62}$$

and from equations 60 and 62 the constant is

$$D = \frac{U_o}{m} + \frac{q(V_s - V_b)}{m} - L\ln r_b. \tag{63}$$

Substituting Equation 63 in 60 yields, after solving for dt,

$$dt = \frac{1}{\sqrt{2L}} \left[\ln \frac{r}{r_b} + \frac{2U_o + 2q(V_s - V_b)}{2Lm} \right]^{-1/2} dr. \tag{64}$$

We further define the constant

$$H = \frac{2U_o + 2q(V_s - V_b)}{m}. \tag{65}$$

and Equation 64 becomes

$$dt = \frac{dr}{\sqrt{2L}\left[\ln r/r_b + H/2L\right]^{1/2}} \tag{66}$$

which is identical in form to Equation 49. One uses the same methods employed in the solution of Equation 49 to obtain

$$T_2 = \frac{r_b e^{H/|2L|}}{\sqrt{|2L|}} \sum_{n=0}^{\infty} \left\{ \frac{(-1)^n}{n!(n+1/2)} \left(\ln r_b/r_c + \frac{H}{|2L|}\right)^{n+1/2} - \left(\frac{H}{|2L|}\right)^{n+1/2} \right\} \tag{67}$$

In the third region between r_c and the collector the equation of motion is

$$m \frac{d^2r}{dt^2} = 0 \tag{68}$$

hence

$$\frac{dr}{dt} = - G \tag{69}$$

where G is a constant velocity. The minus sign is introduced because the radius vector is taken positive in the radial direction whereas the radial velocity is inward toward the collector. We have then

$$T_3 = -\int_{r_c}^{0} \frac{1}{G}\, dr \tag{70}$$

and

$$T_3 = \frac{1}{G} r_c \tag{71}$$

The energy of an ion reaching r_c is

$$\frac{1}{2}mv_0^2 = q(V_s - V_b) + q(V_b - V_c) + U_o \tag{72}$$

but $V_c = 0$, hence

$$\frac{1}{2}mv_c^2 = qV_s + U_o \tag{73}$$

Now

$$G_c = v_c = \left(\frac{2q}{m} V_s + \frac{2U_o}{m}\right)^{1/2} \tag{74}$$

and

$$T_3 = \left(\frac{m}{2qv_s + 2U_o}\right)^{1/2} r_c \tag{75}$$

The total transit time is given by Equation 36 to be

$$T = \frac{r_s \exp\left(\frac{v_0^2}{|2K|}\right)}{\sqrt{|2K|}} \sum_{n=0}^{\infty} \frac{(-1)^n}{n!(n+1/2)} \left\{ \left(\ln r_s/r_b + \frac{v_0^2}{|2K|}\right)^{n+1/2} - \left(\frac{v_0^2}{|2K|}\right)^{n+1/2} \right\} + \frac{r_b \exp(H/|2L|}{\sqrt{|2L|}} \sum_{n=0}^{\infty} \frac{(-1)^n}{n!(n+1/2)}$$

$$\left\{ \left(\ln r_b/r_c + \frac{H}{|2L|}\right)^{n+1/2} - \left(\frac{H}{|2L|}\right)^{n+1/2} \right\}$$

$$+ \left(\frac{m}{2qV_s + 2U_o}\right)^{1/2} r_c \tag{76}$$

It is interesting to examine the space focusing properties of this cylindrical time-of-flight spectrometer. We consider a cylindrical spectrometer with grid radii of 5.08 cm, 4.60 cm, and 4.12 cm. It is assumed that there is no initial velocity spread of ions in the pulsing region. With this condition, Equation 76 reduces to

$$T = \sqrt{\frac{m}{2q}} \left\{ \left(\frac{\ln r_s/r_b}{V_s - V_b}\right)^{1/2} r_s \left\{ \sum_{o}^{\infty} \frac{(-1)^n}{n!(n+1/2)} (\ln r_s/r_b)^{n+1/2} \right\} \right.$$

$$+ \left(\frac{\ln r_s/r_b}{V_b}\right)^{1/2} \left\{ \exp \frac{(V_s-V_b)\ln r_b/r_c}{V_b} \right\} \sum_{n=0}^{\infty} \frac{(-1)^n}{n!n+1/2}$$

$$\left\{ (\ln r_b/r_c + \frac{(V_s-V_b)}{V_b} \ln r_b/r_c)^{n+1/2} \right.$$

$$\left. \left. - \left(\frac{(V_s-V_b)\ln r_b/r_c}{V_b} \right)^{n+1/2} \right\} + \left(\frac{1}{V_s}\right)^{1/2} r_c \right\}. \qquad (77)$$

Using the boundary conditions that at $r=r_a$, $V=V_a$ and at $r=r_b$, $V=V_b$, with Equation 19, it can be seen that V_a is related to V_s by

$$V_s = V_a - \frac{(V_a-V_b)}{\ln r_a/r_b} \ln r_a/r_s \qquad (78)$$

A digital computer program was developed to investigate the time spread between three ions of the same charge to mass ratio but different values of r_s. The values of

r_s chosen for the three ions were 5.00 cm, 4.84 cm, and 4.68 cm respectively. One defines the following time differences

$$\Delta T_1 = T_1 - T_2 \tag{79}$$

$$\Delta T_2 = T_2 - T_3 \tag{80}$$

$$\Delta T_3 = T_1 - T_3 \tag{81}$$

where T_1, T_2, and T_3 are the total times each respective ion takes to traverse the spectrometer for a given value of V_a and V_b. Equation 81 therefore yields the approximate width of the recorded mass peak. It follows that if space focusing is to occur there should be a minimum in the absolute values of ΔT_1, ΔT_2, and ΔT_3 for some value of the ratio V_a/V_b. Figure 4 shows a computer plot of each time difference versus V_a/V_b. The minimum occurs at a ratio of 1.85/1 for ΔT_3. The graph of Figure 4 indicates a sharper focus than the graph of Figure 3 for the linear spectrometer of the same dimensions. Hence the space focus condition is more critical for the cylindrical spectrometer.

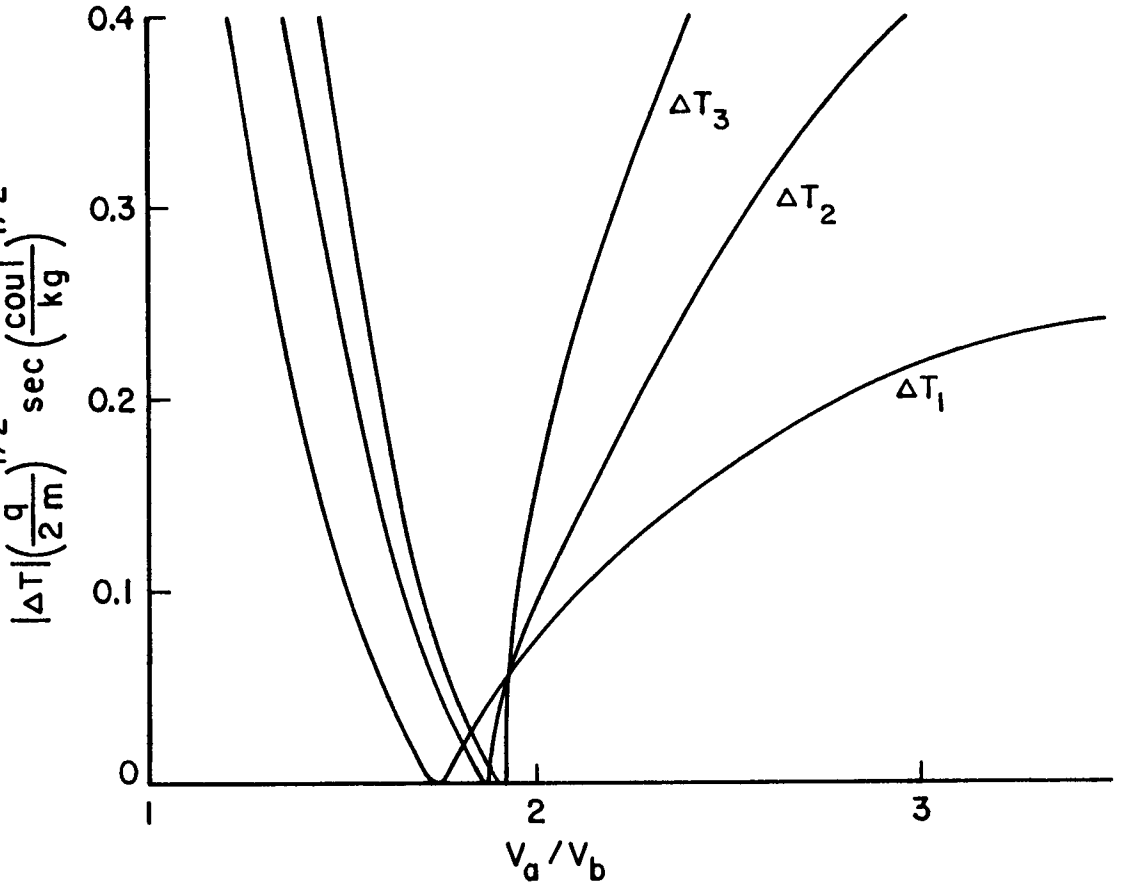

SPACE FOCUSING OF THE PROPOSED CYLINDRICAL PULSED-BEAM MASS SPECTROMETER

FIGURE 4

3.3 A Time-of-Flight Mass Spectrometer of Wedge Shaped Geometry

Figure 5 illustrates a pulsed-beam mass spectrometer of wedge shaped geometry which may be considered a segment of the cylindrical spectrometer considered above. The development preceding this section may be considered a valid approximation to the wedge spectrometer provided the following conditions obtain. The radius of each individual grid must be much larger than the difference in the radii of successive grids. This insures that the fringing fields in the gaps near the edges of the grids may be validly neglected. The angle of the wedge should be sufficiently large to insure that the fields existing in the wedge are close to those which exist in the full cylinder.

The particular wedge spectrometer constructed for this work differs from the Wiley and McLaren instrument not only in geometry but also in the method of ion introduction. In this instrument the ions are formed externally and are injected into the pulsing region instead of being formed directly in the pulsing region. Once the ions are introduced into the spectrometer a pulse is applied to grid 1. The ions are accelerated by this pulse into the region between 2 and 3 and eventually reach the field free region between 3 and the collector. The grid 3 is held at ground potential as is the grid 4

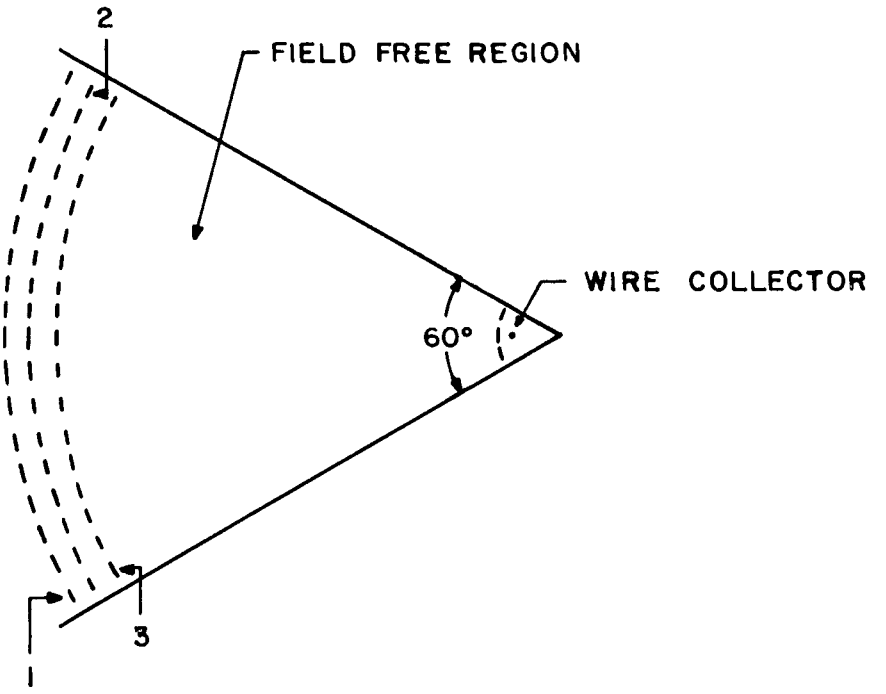

UNGATED WEDGE SPECTROMETER

FIGURE 5

which insures that no charge will be induced on the collector before the ions pass through grid 4. At the energies involved in this spectrometer (less than 100 volts), the effects of secondary electrons are negligible.

Since all the ions leave the source region with constant energy but different mass to charge ratios they are separated in time according to Equation 76 above. Hence each ion bunch homogeneous in mass to charge ratio requires a unique transit time. The signal received at the collector is amplified and displayed on an oscilloscope whose internal time base is triggered by the initial accelerating pulse. In this manner a mass spectrum of the ions under investigation is obtained.

In actual practice the spectrometer of Figure 5 was the first version to be tested. It was thought that the focusing of the ion bunches would be adequate to obtain a detectable signal at the collector. The wire collector has the advantage of having a small capacitance. It was found by experimental and theoretical considerations that the focusing was not adequate to deliver a sufficient signal to the amplifiers involved in the collector circuit.

This problem was circumvented by the following methods. The collector was greatly enlarged in order to intercept a much greater percentage of the ion current than the wire. A gating system was added in order to

permit the use of a limited response electrometer amplifier. This nullifies the advantage of being able to sweep a complete spectrum very rapidly but yields the possibility of employing an instrument which is capable of detecting currents of 10^{-14} Amperes or less. Other modifications included the addition of metal plates to the top and bottom and both sides of the wedge. It was possible to supply dc potentials to these plates to improve the ion focusing capability of the instrument. The plates were arranged such that the appropriate potentials would cause a focusing action toward the collector. All the modifications mentioned above were incorporated in such a fashion that the instrument could be operated in either a gated or ungated mode.

3.4 Working Principle of Wedge Spectrometer in the Ungated Mode

Figures 6 and 7 illustrate the modifications made to the original spectrometer. If one grounds the grids 4, 5, and 6 the spectrometer becomes identical with the original except for the enlarged collector and the focusing plates. The grids 1, 2, and 3 serve the same functions as explained in the preceding section. An example of the type of data obtained with this system will be given later.

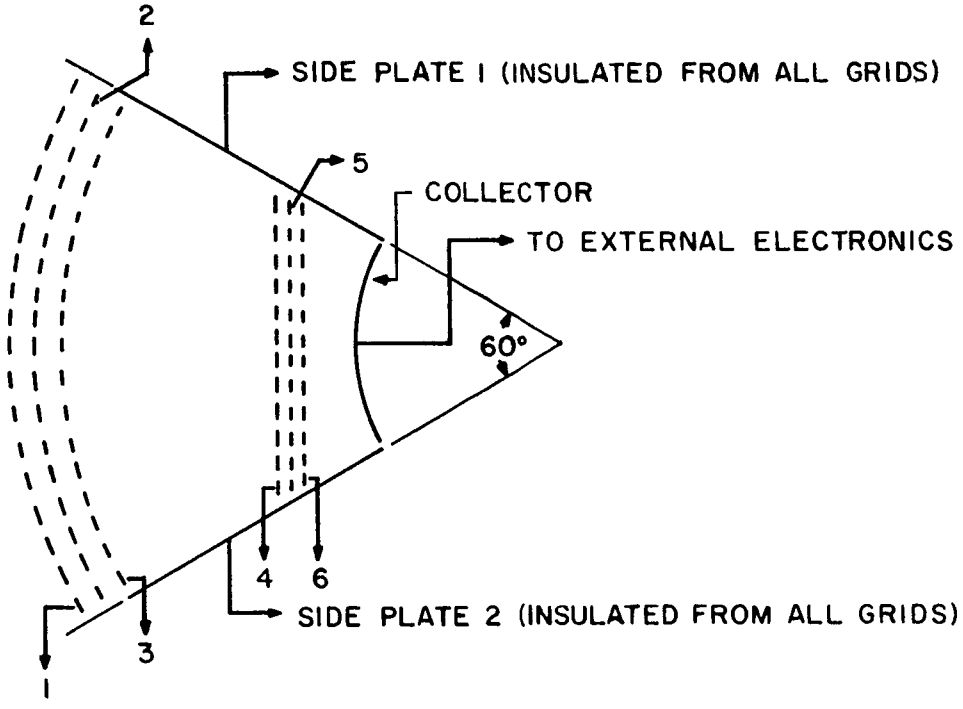

GATED WEDGE TIME OF FLIGHT
MASS SPECTROMETER (TOP VIEW)
FIGURE 6

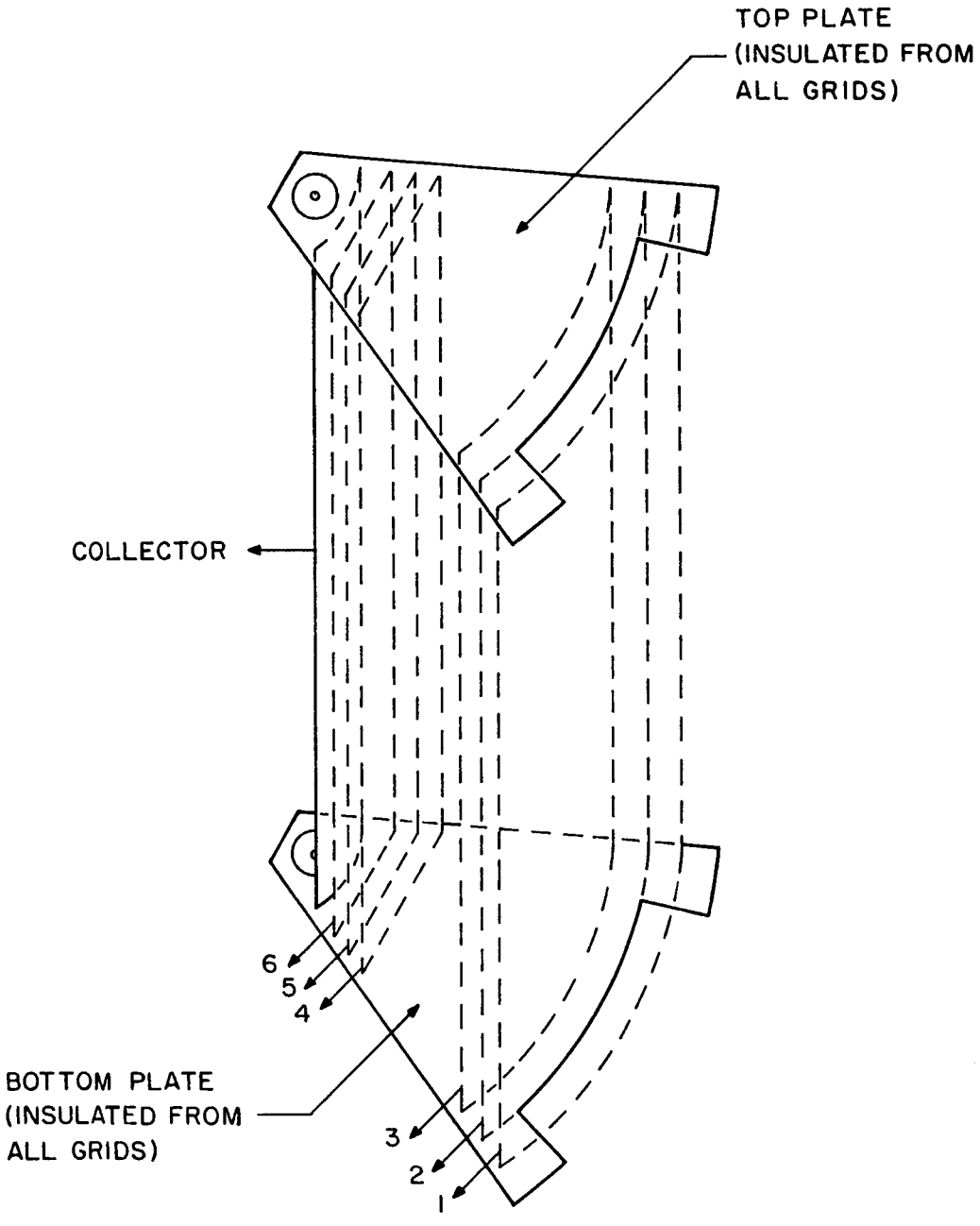

GATED WEDGE TIME OF FLIGHT MASS SPECTROMETER

FIGURE 7

3.5 Working Principle of the Wedge Spectrometer in the Gated Mode

The ions under investigation may be injected into the wedge spectrometer by one of two methods. The first method consists of injecting the ions into the pulsing region directly through the grid 1 at a ninety degree angle to the collector. The second method consists of injecting the ions between 1 and 2 parallel to the collector. Grids 1 and 2 are both held at the same dc bias voltage while the pulse is superimposed on 1. The grids 3, 4, and 6 are held at ground potential.

The grids 4, 5, and 6 constitute an ion gate. The grid 5 is held at a dv voltage comparable with the energy given to the ion bunch in the pulsing region. At the appropriate time a gate is lowered by means of a very short duration pulse applied to 5. This gate pulse is delayed in time from the initial accelerating pulse by an amount of time which exactly equals the time of flight of a group of ions of one particular mass to charge ratio. It is necessary for the gate pulse to be as sharp as possible, typically 50 nanoseconds, in order to insure that only ions of one particular mass to charge ratio reach the collector. A long duration gate pulse will cause poor resolution. The grids 4 and 6 are grounded in order to prevent field penetration into the region between 6 and the collector and into the zero field region

between 3 and 4, the ion flight path. The potentials of grids 1 and 2 are adjusted such that the ions are actually focused at the gate grid.

In addition to the actual grids involved in the control of the ion bunch, the final version of the spectrometer includes side plates as illustrated in Figure 6 and top and bottom plates as illustrated in Figure 7 (only the top plate is illustrated in Figure 7). These plates are insulated from all grids. By means of appropriate potentials applied to the side and top plates it is possible to improve the focusing of the ions impinging on the gate, as mentioned earlier.

CHAPTER IV

EXPERIMENTAL APPARATUS

4.1 Description of the Ionization Sources

One of the ion sources used in testing the wedge spectrometer was a surface ionization source similar to the type described by Kendall and Luther (1966). A platinum button 0.3 cm in diameter was spotwelded onto a tungsten filament in order to provide an equipotential surface from which ions could be emitted. The filament itself was heated by an alternating current and held at a fixed dc potential. This source may be charged with any one of a number of salts, including sodium and potassium. The salt is placed in solution with water and the button is heated to about 180 degrees Centigrade via infra-red lamps. A drop of the charging solution is placed on the button and the water is flashed off leaving a fine dust of the salt on the button.

The other type of source used in the analysis of gas samples was a standard electron bombardment source. The ions are formed by collisons between gas molecules and an electron beam. These ions are continuously ejected from the ionization region by an appropriate repelling potential.

4.2 Description of the Wedge Spectrometer

The dimensions of the spectrometer illustrated in Figures 6 and 7 are tabulated in Table 1 below.

Table 1

Grid Spacings of the Wedge Spectrometer

Grid Region	Distance of Separation (cm)
1-2	0.477
2-3	0.477
3-4	1.570
4-5	0.310
5-6	0.310
6-Collector	1.900

The radius of the instrument is 5.08 cm as measured from the collector to the outer grid. All grids are mounted on mica insulators and the grid material itself is woven tungsten mesh which contains 80 holes per inch.

4.3 Electronics of the Ungated Wedge Spectrometer

Figure 8 illustrates a block diagram of the electronics used when the grids 4, 5, and 6 are held at ground potential. This mode of operation renders the gate inoperative and provides a region of zero electric field between 3 and the collector. The pulsed grid, 1, is held at a constant dc bias voltage via the voltage

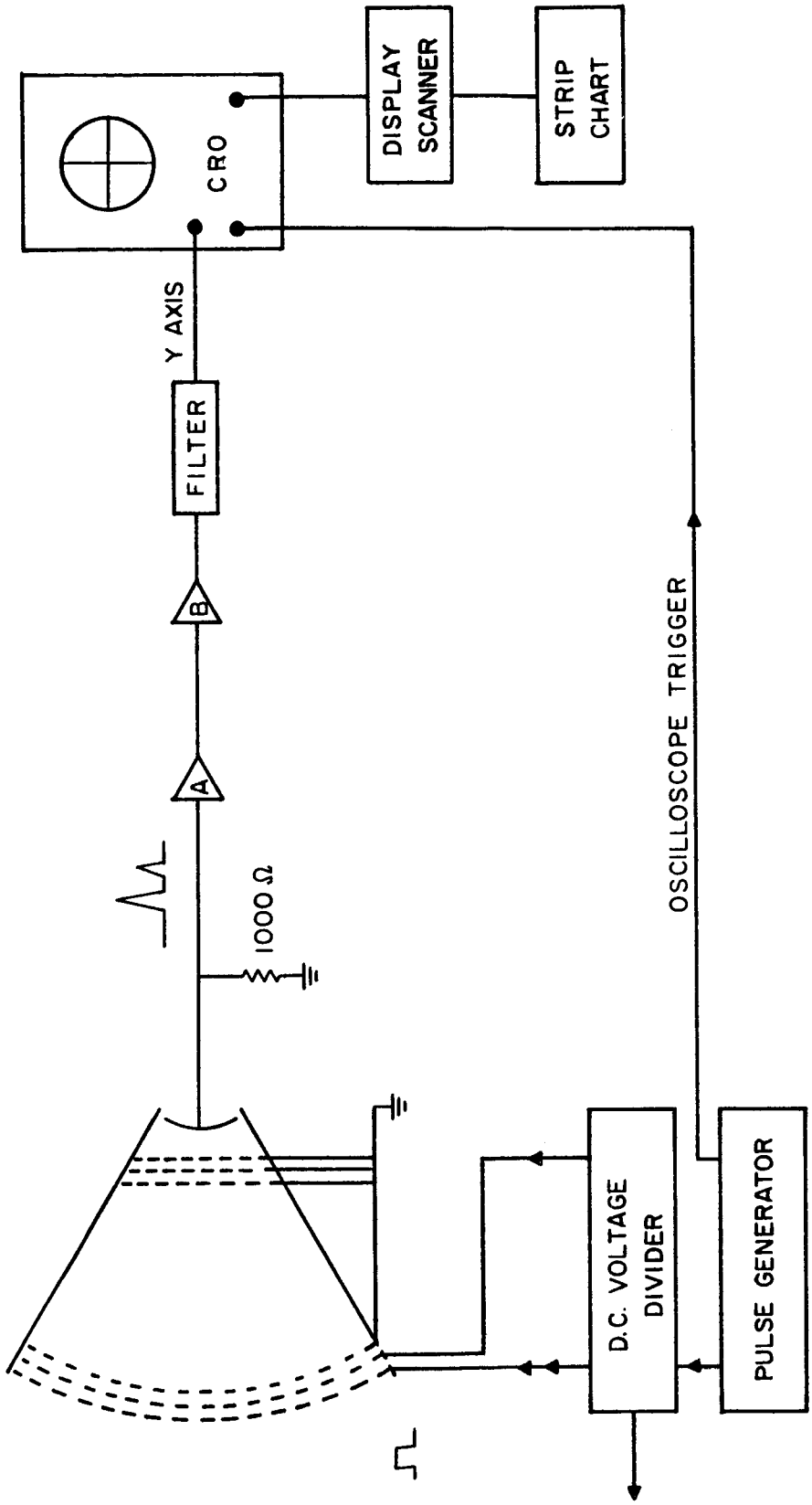

ELECTRONICS OF THE UNGATED WEDGE SPECTROMETER
FIGURE 8

divider network which also supplies a dc voltage to grid 2 and the top and side plates. The signal the collector receives creates a voltage drop across the 1000 Ohm resistor. The two amplifiers, A and B, are fast rise preamplifiers with a maximum risetime of 6 nanoseconds and an input impedance of one Megohm. These amplifiers are operated in such a fashion that the total gain of the system, including amplifiers A, B, and the oscilloscope preamplifier is approximately 1000. This indicates that the detector current which would cause a one centimeter deflection on the oscilloscope is about 5×10^{-9} Amperes. The value of resistance used is the maximum allowable for good frequency response. The detected and amplified signal is fed through a high pass filter in order to eliminate low frequency noise from the mains. This filtered signal is then displayed on the vertical axis of the oscilloscope. The horizontal axis of the oscilloscope is controlled by the internal time base circuitry which is triggered by a signal from the pulse generator. The triggering signal occurs at the same time as the accelerating pulse applied to grid 1.

The oscilloscope was equipped with a display scanner which made possible a graphical record of the mass spectrum in addition to the visual read-out of the cathode ray tube itself. An example of the type of data obtained in this mode of operation will be given in a

later section.

4.4 Electronics of the Gated Wedge Spectrometer

Figure 9 is a block diagram of the electronics associated with the wedge spectrometer when it is operated in the gated mode. Pulse generator A supplies the ion accelerating pulse to grid 1 and at the same time triggers pulse generator B. The pulse generated by B may be delayed in time from the initial accelerating pulse by means of a variable delay. The delay is controlled by a mechanical drive system consisting of a variable speed motor which turns the wiper of a ten turn linear potentiometer whose resistance is 500 Ohms. The delayed pulse is differentiated and the positive part of the differentiated pulse is clipped by a diode. This differentiation and clipping is performed in order to reduce the width at half height of the delay pulse to 50 nanoseconds. This short duration negative pulse is applied to grid 5 at an appropriate time to permit one ion bunch homogeneous in mass to charge ratio through the gate to the collector. All other ion bunches are blocked by the dc barrier on grid 5. It is possible by means of the dc voltage divider to supply a potential to both 1 and 2, as well as the gate grid 5. The gate pulse swings negative from the positive barrier potential in order to let the appropriate ion bunch reach the collector

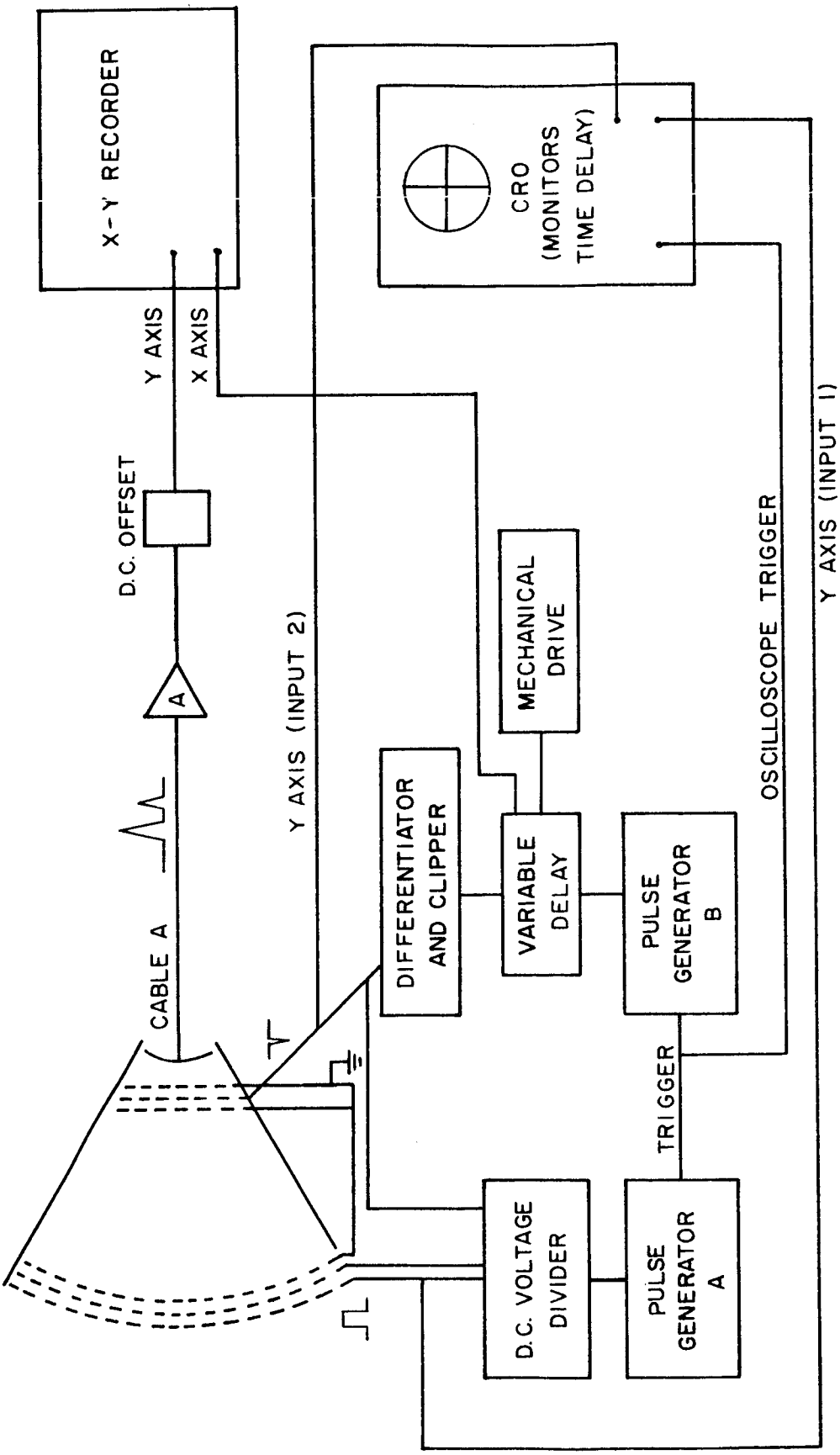

ELECTRONICS OF THE GATED WEDGE SPECTROMETER

FIGURE 9

The signal is then fed to an electrometer through a special low noise cable marked cable A in Figure 9. This cable has a graphite coating on the insulation between the central conductor and the braided shield which helps eliminate extraneous signals due to mechanical flexing of the cable. The electrometer, A, which has an input impedance of 10^{15} Ohms, is used to monitor the current at the collector. It amplifies the signal and feeds it into the Y axis of the X-Y recorder. A dc offset is used to control the effective dc level of the electrometer.

The X axis of the recorder is controlled by the voltage developed across the variable resistor which controls the delay of the gate pulse. Hence the X axis of the recorder may be given a time calibration by monitoring the time difference between the ion accelerating pulse and the delayed gate pulse.

Both the accelerating pulse and the gate pulse are monitored by a dual trace preamplifier in the oscilloscope. The horizontal axis of the oscilloscope is controlled by the internal time base circuitry and the sweep is triggered by the same signal that triggers pulse generator B.

CHAPTER V

EXPERIMENTAL RESULTS[1]

5.1.0 Mass Spectra Obtained With the Ungated Spectrometer

The ungated spectrometer, illustrated in Figure 8, was used to obtain the spectrum appearing in Figure 10. This data was obtained using the surface ionization source described earlier. The source had been charged with a mixture of sodium and potassium salts. The ions were injected directly through grid 1 with an energy of 4 eV. Grid 1 held a dc potential of 20 V upon which was superimposed a pulse of height 20 V and width 0.5 microseconds. The pulses were applied at grid 1 at the rate of 100 Kc per second. The grid 2 was held at 20 V dc and both side plates were held at 50 V dc while the top and bottom plates had a potential of 200 V.

5.2.0 Mass Spectra Obtained With the Gated Spectrometer

Figures 11 and 12 illustrate typical data taken with the gated spectrometer and surface ionization source. Both spectra were produced under identical conditions except that in Figure 11 all focusing plates were maintained at zero volts whereas in Figure 12 the side plates were maintained at 200 Volts. The improvement in resolving power can be seen as the individual sodium and potassium peaks are almost completely resolved.

[1]The data illustrated in this section of the thesis was taken in conjunction with Martin F. Zabielski of the Ionosphere Research Laboratory, Penn State University.

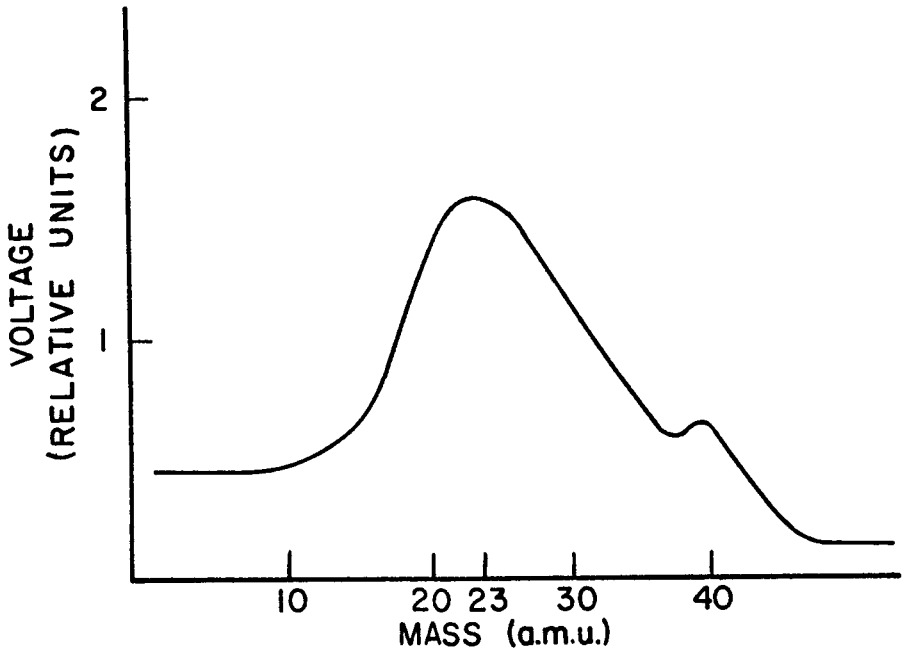

MASS SPECTRUM OF $^{23}Na^+$, $^{39}K^+$, $^{41}K^+$
FROM UNGATED SPECTROMETER

FIGURE 10

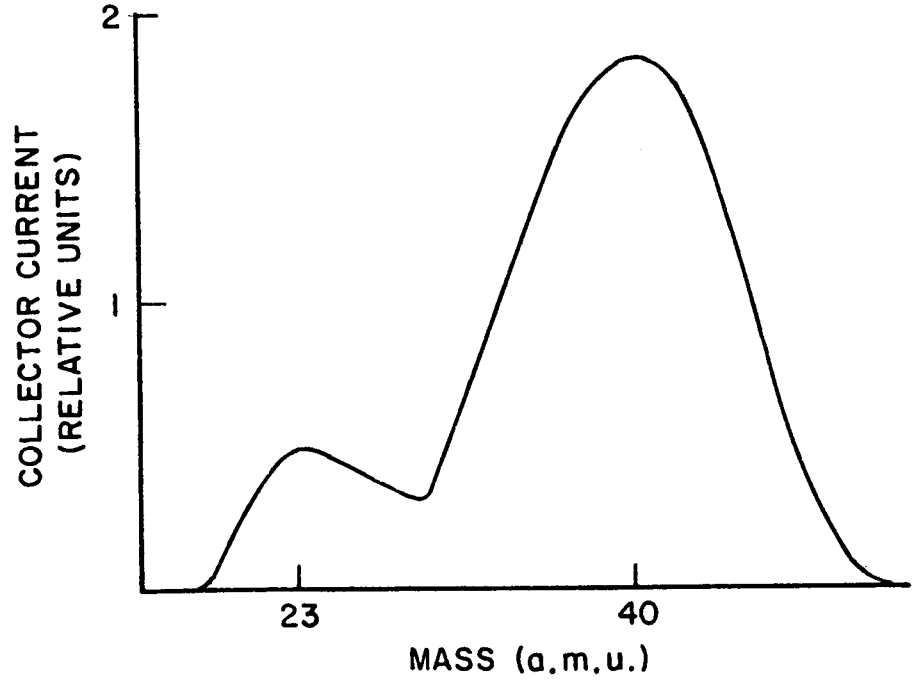

MASS SPECTRUM OF $^{23}Na^+$, $^{39}K^+$, $^{41}K^+$, FROM GATED SPECTROMETER
(DIFFERENT SAMPLE FROM THAT USED IN FIGURE 10)

FIGURE 11

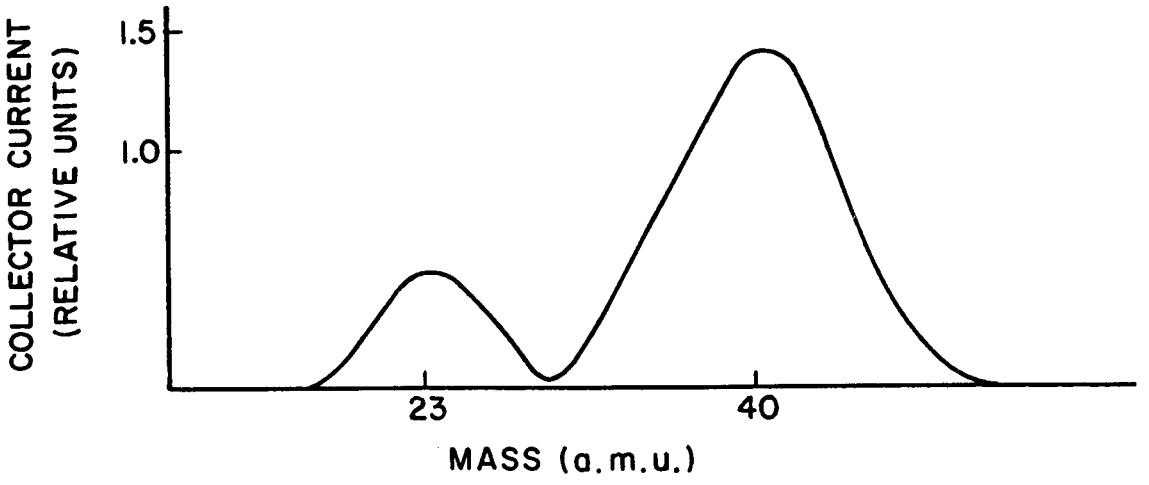

MASS SPECTRUM OF $^{23}Na^{+}$, $^{39}K^{+}$, $^{41}K^{+}$, FROM GATED SPECTROMETER WITH FOCUSING PLATES

FIGURE 12

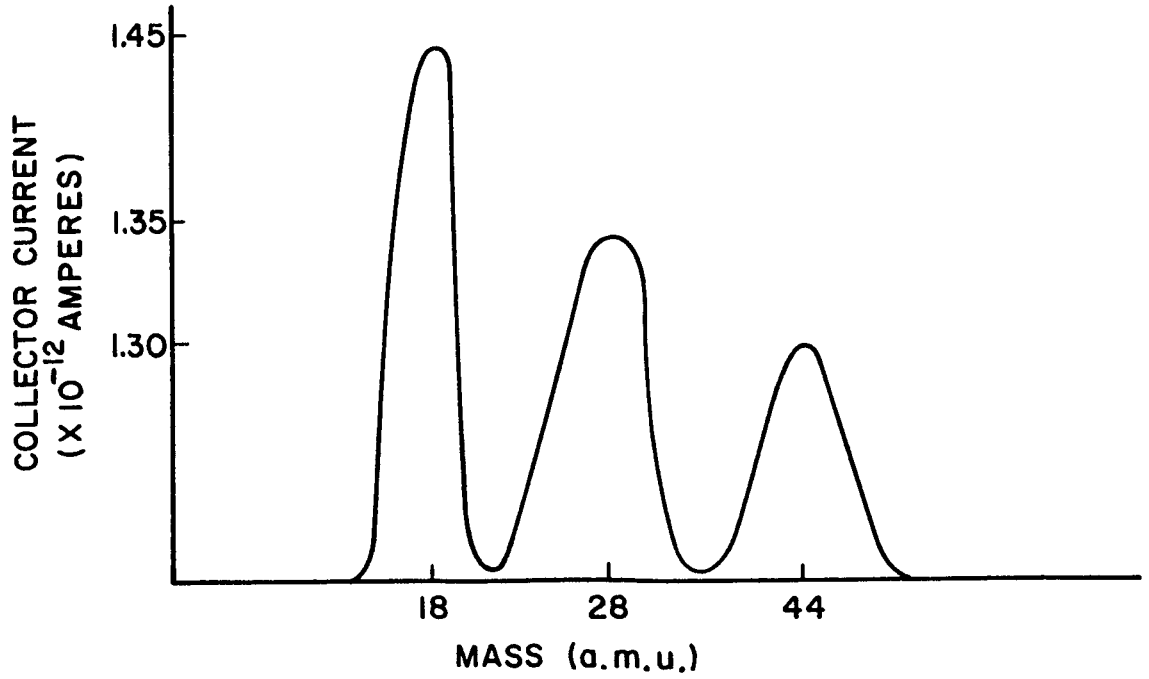

RESIDUAL GAS SPECTRUM FROM GATED SPECTROMETER

FIGURE 13

The data illustrated in Figures 11 and 12 was obtained by forcing the ions into the pulsing region directly through grid 1. The ions entered the spectrometer with an energy of 9 eV. Grids 1 and 2 were maintained at a dc potential of 15 V and a pulse of height 20 V and width 0.4 microseconds was superimposed upon the dc bias of grid 1. The pulse repetition rate was 100 Kc per second and the gate grid was maintained at 22 V dc. A pulse of amplitude -18 V and width 50 nanoseconds worked downward from this dc level. The typical peak heights of the potassium in Figures 11 and 12 were $7x10^{-11}$ Amperes. All data illustrated thus far was taken at pressures around $5x10^{-7}$ Torr.

5.2.1 Residual Gas Analysis Using the Gated Spectrometer and Electron Bombardment Source

Figure 13 illustrates a residual gas analysis performed in conjunction with an electron bombardment ionization source. In this case the ions were introduced into the pulsing region between grids 1 and 2 on a line parallel to the collector with an energy of 100 eV. The grid 1 had a pulse of 90 V height and 1 microsecond width superimposed upon a dc potential of 45 V. Grid 2 was held at 50 V dc. The gate had a potential of 110 V and the gate pulse dropped from this value -38 V. The repetition rate was 30 Kc per second. The top and

bottom plates were maintained at ground potential while the side plates each operated at 150 V. The chamber pressure was maintained at 2×10^{-6} Torr as measured by a nude Bayard-Alpert ionization gauge.

5.2.2 High Pressure Operation

A series of tests were performed on the gated spectrometer in order to find the maximum pressure at which the instrument could function. The source used in these tests was the surface ionization source which injected the ions into the spectrometer between grids 1 and 2. The instrument was tested under pressures ranging from 10^{-7} Torr to 50 microns. Instrument performance did not deteriorate until the pressure had reached 50 microns.

It will be noted here that the upper pressure limit, 50 microns, is a conservative estimate of the maximum operating pressure. The reason for this can be found in the manner in which the ions were injected into the spectrometer. The ion beam had to travel a distance comparable to the length of the ion flight path of the spectrometer before they entered the pulsing region. It is possible that much of the deterioration of the instrument performance was due to the scattering of ions by residual gas molecules before they actually entered the pulsing region of the spectrometer. This is partially

verified by the fact that the instrument sensitivity was sharply reduced at the upper pressure of 50 microns. It would appear that only a small percentage of the ions leaving the source were actually entering the pulsing region.

Pressures in the range of 10^{-7} Torr to 10^{-4} Torr were measured by a nude Bayard-Alpert gauge located in the evacuated chamber whereas pressures in the range 1 micron to 50 microns were measured by a thermocouple gauge located at the same place.

5.2.3 Calibration of the Mass Scale

An experimental calibration of the wedge spectrometer was performed in order to determine the time required for an ion of a given mass to charge ratio to traverse the spectrometer. This was accomplished by introducing various gas samples, one at a time, into the vacuum chamber and performing a sweep of the mass spectrum. The ionizing agent was the electron bombardment source. Figure 14 illustrates a typical spectrum obtained when oxygen was introduced into the chamber. The first peak observed is H_2O^+ which is present because of the water content of the atmosphere in the vacuum chamber. The second peak is the oxygen peak. (About five percent of the O_2 molecules present in the evacuated chamber will fracture under electron

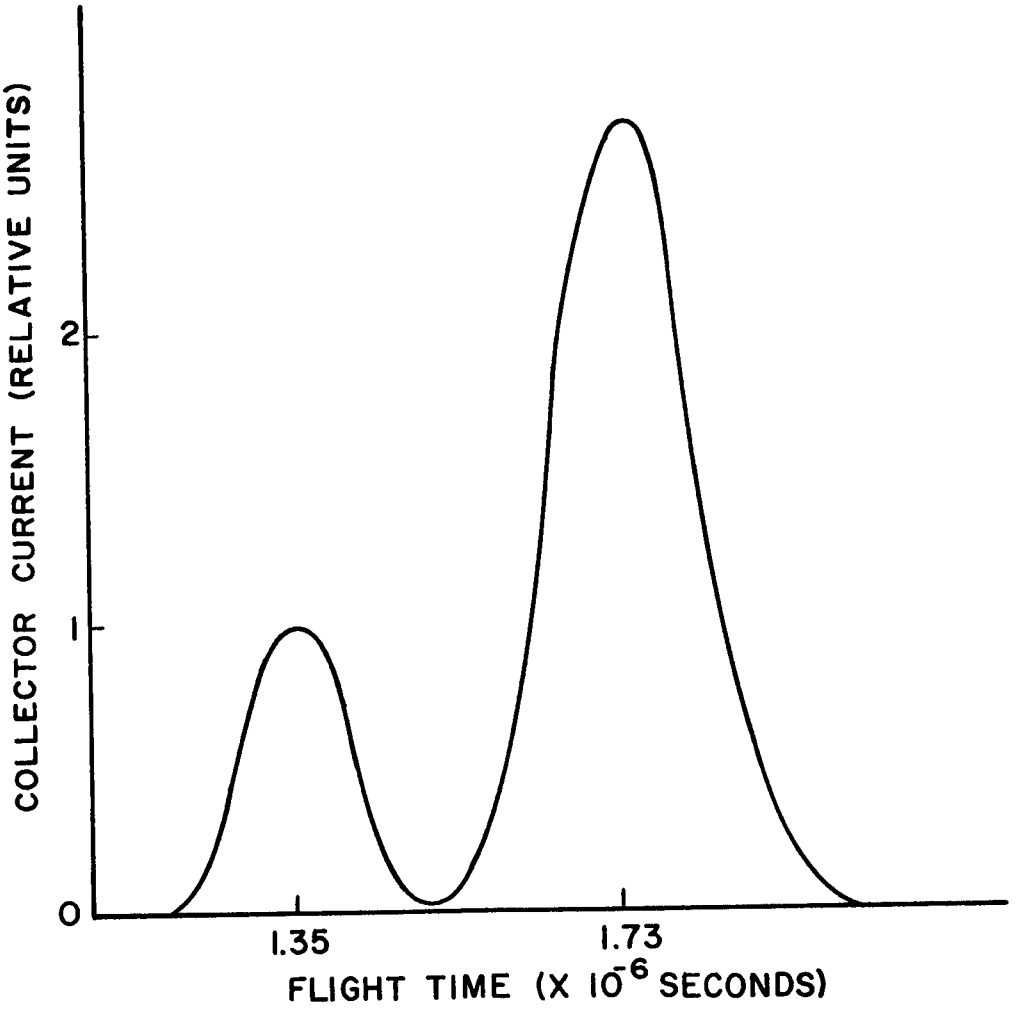

TIME CALIBRATION MASS SPECTRUM

FIGURE 14

bombardment and form 0^+ which has a mass of 16 amu. Since the spectrometer's resolving power is not great enough to resolve individual peaks at mass 16 amu and 18 amu, the peak occurring at 1.35 microseconds in Figure 14 is a combination of 0^+ and H_20^+). This type of analysis was performed with Ne, 0_2, CO_2, and X_e. Flight times were obtained for all these gas samples under similar conditions. The mass range covered stems from 18 amu to 131 amu but the majority of gas samples used were in the range from 18 amu to 44 amu. This is predominantly the mass range of the ions found in the lower ionosphere.

Figure 15 is a plot of the square root of the mass versus flight time for ions in the mass range between 18 amu and 131 amu. It can be seen that the flight time varies in proportion to the square root of the mass as is to be expected of an instrument of this nature.

5.3.0 Resolving Power and Sensitivity

One way of defining resolving power is that the resolving power at mass m, R_m, is

$$R_m = \frac{m}{\Delta m} \tag{82}$$

where Δm is the width at half height of the mass peak at mass m. If one uses this definition in application to the Figures 11, 12, and 13 of this thesis one finds

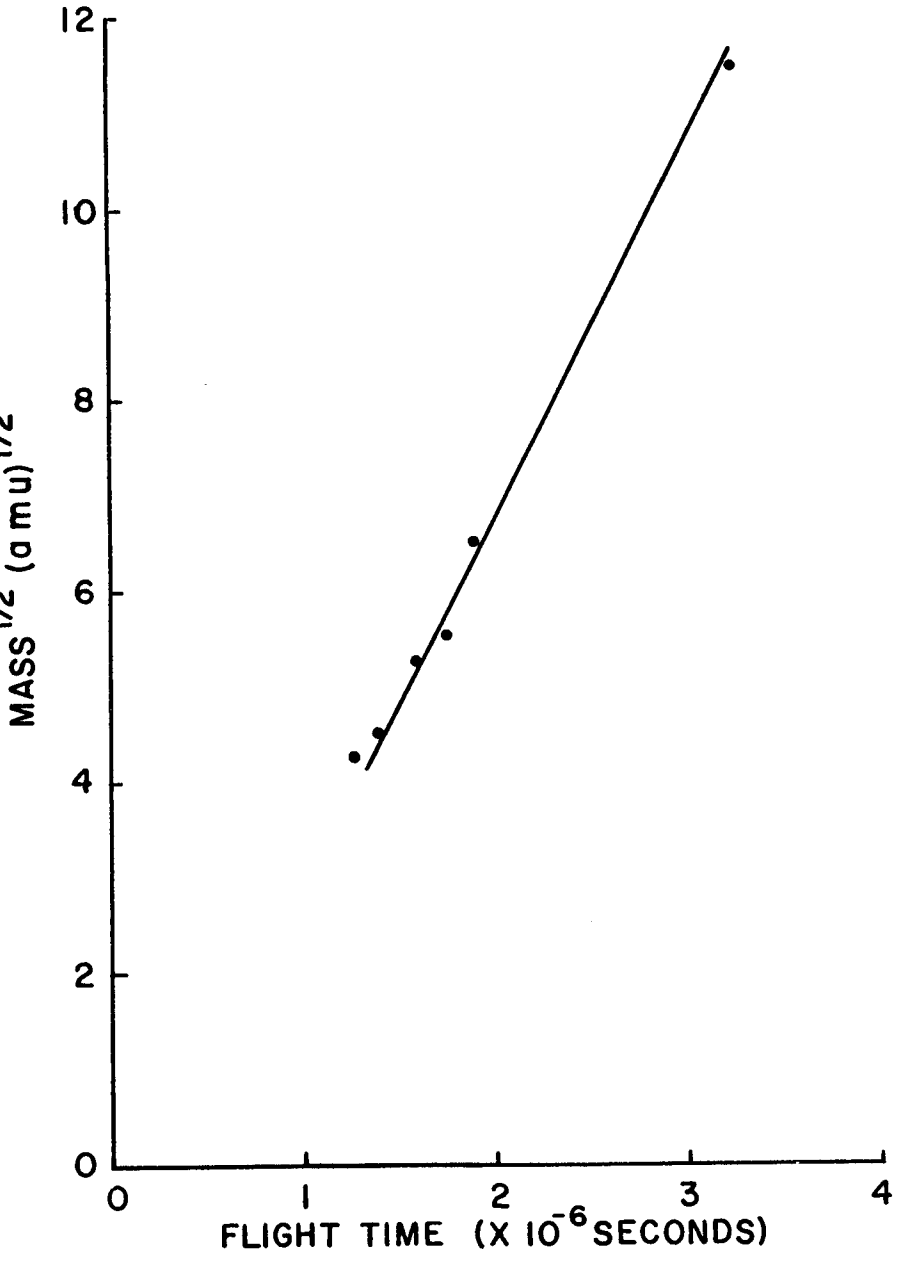

EXPERIMENTAL TIME CALIBRATIONS OF THE WEDGE SPECTROMETER

FIGURE 15

the following.

Figure 11 yields a resolving power of slightly less than 2 whereas Figure 12 illustrates a resolving power of slightly over 3. This demonstrates the slight increase in resolving power due to the additional focusing action of the focusing plates of the wedge spectrometer.

Figure 13, the first residual gas spectrum, illustrates a resolving power of about 6 at mass 18. It appears at the present state of development that a resolving power of from 6 to 10 is about the best that is to be expected from this particular version of the wedge spectrometer. However, as mentioned earlier, there is a possibility that this spectrometer can be used with proper data processing techniques to yield a resolving power of 60 or more.

Although the wedge spectrometer is a low resolution device, the sensitivity of the instrument is quite high. If one assumes singly charged ions of one particular mass are contained in the pulsing region, the average current collected is

$$I_{ave} = \frac{\Delta q}{\Delta t} \tag{83}$$

where Δq is the amount of charge originally contained in the pulsing region and Δt is the time interval between pulses. The pulse repetition rate was typically 30Kc per

second. If we assume that the pulsing region completely refills with ions after each pulse and the electrometer used to monitor the gated collector current can detect 10^{-12} Amperes then Δq is approximately 3.3×10^{-17} Coulombs. Since the volume of the pulsing region is 7.2 cubic centimeters, the number density of particles needed to observe a detectable mass peak is about 29 ions per cubic centimeter. This is well within the sensitivity required in ionospheric investigations.

CHAPTER VI

CONCLUSIONS

6.1 Problems Encountered in Recording Mass Spectra

The main problem encountered in obtaining mass spectra with the gated spectrometer was elimination of a constant ion current which penetrated the gate barrier at all times. This constant ion current is a consequence of the basic construction of the instrument. It is possible for the ions to travel around the barrier grid because of rather large constructional gaps between the gate grid and the top and side plates. Hence a finite current arrived at the collector regardless of the magnitude of the potential barrier.

Another problem encountered was the gate pulse itself. In order to obtain a short duration gate pulse it was necessary to differentiate the output of the gate pulse generator and then clip the unwanted portion of the differentiated pulse by means of a diode. This process severely attenuates the magnitude of the final gate pulse. It was found, however, that the gate pulse was of sufficient height to let the majority of ions of selected mass through to the collector.

6.2 Suggested Improvements

The resolving power of the gated wedge spectrometer may be increased by moving the grids 4, 5, and 6 closer

to the collector. This will increase the overall ion flight path and thereby increase the resolving power. It is thought that this modification will not severely hamper the instruments ability to operate at high pressures. It is also possible to reduce the distances between the grids of the gate system. This will reduce the amount of time taken to gate an ion bunch.

The first dynode of an electron multiplier could be used as the collector which would increase the sensitivity of the spectrometer. This may hamper the spectrometer's high pressure performance because of possible arcing between multiplier dynodes.

6.3 Summary

The analysis of the wedge time-of-flight mass spectrometer has shown that it can be an effective tool in determining the ion composition of the upper atmosphere. The instrument's ability to operate at high pressures along with its high sensitivity make feasible both positive and negative ion investigations in the D and E regions of the ionosphere. The spectrometer will require no external pumping and it may be flown on small inexpensive rockets.

BIBLIOGRAPHY

1. Agishev, E. I. and N. I. Ionov, Sov. Phys.-Tech. Phys, 1, 201 (1956).

2. Borovik, E. S. and S. F. Grishin, Sov. Phys.-Tech. Phys., 4, 1014 (1959).

3. Cameron, A. E. and D. F. Eggers, Rev. Sci. Instr., 19, 605 (1948).

4. Glenn, W. E., UCRL-1511 (October 1951).

5. Glenn, W. E., AECD-3337, (UCRL-1628) (January 1952).

6. Hoffman, J. H., Thirteenth Annual Conference on Mass Spectrometry and Allied Topics, St. Louis, 327 (1965).

7. Ionov, N. I. and B. A. Mamyrin, J. Tech. Phys. (USSR), 23, 2101 (1953).

8. Johnson, C. Y. and J. P. Heppner, J. Geophys. Res., 60, 193 (1955).

9. Johnson, C. Y. and E. B. Meadows, J. Geophys. Res., 60, 193 (1955).

10. Johnson, C. Y., E. B. Meadows, and J. C. Holmes, J. Geophys. Res., 63, 443 (1958).

11. Johnson, C. Y., et. al., J. Geophys. Res., 14, 475 (1958).

12. Katzenstein, H. S., and S. S. Friedland, Rev. Sci. Instr., 26, 324 (1955).

13. Keller, R., Helv. Phys. Acta., 22, 386 (1949).

14. Kendall, B.R.F., Rev. Sci. Instr., 32, 758 (1961).

15. Kendall, B.R.F., Rev. Sci. Instr., 33, 30 (1962).

16. Kendall, B.R.F., Jour. Sci. Instr., 39, 267 (1962).

17. Kendall, B.R.F., Jour. Sci. Instr., 43, 215 (1966).

18. Kendall, B.R.F. and H. M. Luther, Am. Jour. Phys., 34, 580 (1966).

19. MacKenzie, E. C., "The Investigation of Ionospheric Electron Density and Ion Composition Using Rocket-Borne Probes," Electron Physics Dept., University of Birmingham, London, Ph.D. Thesis (1964).

20. Narcisi, R. S., and A. D. Bailey, J. Geophys. Res., 70, 2687 (1965).

21. Nier, A. O., Thirteenth Annual Conference on Mass Spectrometry and Allied Topics, St. Louis, 281 (1965).

22. Sakseev, D. A., Prib. i Tekh Eksper, No. 6, Nov.-Dec., 135 (1965).

23. Sayers, J., Proc. Royal Soc. Lon., 253, 522 (1959).

24. Schaefer, E. J., J. Geophys. Res., 68, 1175, (1963).

25. Stephens, W. E., Bull. Am. Phys. Soc., 21 (1946).

26. Takekoshi, H., K. Tsuroka and S. Shimizer, Bull. Inst. Chem. Res., Kyoto Univ. 27, 52 (1951).

27. Wiley, W. C. and I. H. McLaren, Rev. Sci. Instr. 26, 1150 (1955).

28. Wolff, M. M., and W. E. Stephens, Rev. Sci. Instr., 24, 616 (1953).

29. Zabielski, M. F., Scientific Report No. 280, Ionosphere Research Laboratory, Penna. State University (1966).